A 2.45 GHz FSS Loaded Rectifying Antenna

UDAYABHASKAR PATTAPU (uday.pattapu@hotmail.com)
Indian Institute of Technology (Indian School of Mines): Indian Institute of Technology
https://orcid.org/0000-0001-9884-6968
Sushrut Das
Indian Institute of Technology (Indian School of Mines): Indian Institute of Technology

Research Article

Keywords: Rectenna, RF-DC conversion efficiency, rectifier, spurious free antenna, wireless power transmission.

Posted Date: September 21st, 2021

DOI: https://doi.org/10.21203/rs.3.rs-755066/v1

Abstract

In this paper the development of a rectenna system has been presented for 2.45 GHz wireless power transfer application. The receiving element of the rectenna (or the antenna) has been designed to possess spurious free response at least up to 10 GHz to improve the RF-DC conversion efficiency. It was found that the gain of the antenna is not sufficient for rectenna application. Therefore, to improve the gain of the antenna, it has been loaded with an angle and polarization insensitive FSS. The FSS loaded antenna achieved 7.7 dB gain, 85% radiation efficiency, and single operating band at 2.45 GHz; which is suitable for developing a rectenna for wireless power transfer. To convert the received RF energy into DC voltage a 2.45 GHz matched rectifier circuit has been designed. L-type matching network has been used to match the complex rectifier impedance with the 50 Ω antenna impedance. 1.52 V output voltage was obtained for 7 dBm input power and 3 kΩ load. Achieved maximum efficiency is 66.13% for 1.1 mW received power. It has been shown that the FSS loading of the antenna has the capacity of drastically improve the efficiency of the rectenna system.

1 Introduction

Rectifying antenna, or rectenna, generally consists of antenna, filter, matching circuit, rectifier, DC pass filter, and load [1]. The rectifier can produce unintended frequencies, which may couple to the antenna and cause interference with nearby RF devices, distortion of received signal, and reduction of efficiency. Therefore, a filter is used [2]. But it increases size and insertion loss. Therefore, spurious free antennas are preferred. High gain is also required for receiving low power.

Suppression of spurious bands and simultaneously increasing antenna gain is an existing challenge. Many techniques have been introduced for suppression of spurious bands, such as, use of defected ground structure (DGS) [3], photonic band-gap (PBG) [4], combined DGS and PBG structures [5], ground slots [6], stubs at the feed line [7], compact microstrip resonant cell [8], printed lowpass filtering antenna [9] and right angle slits embedded in the antenna [10] etc. For improvement of gain artificial magnetic conductor (AMC) [11] and frequency selective surfaces (FSS) have been used [12]-[14].

Rectenna design was first proposed by Brown [15]. He designed a rectenna at 2.45 GHz. He also developed a 35 GHz rectenna with 33% conversion efficiency (CE) [16]. Hong [17] reported a rectifying antenna using a finite ground CPW circuit which had 68.5% CE for 270 Ω load. Riviere [18] proposed a rectenna circuit at 2.45 GHz for low input power. Maximum CE was 34% for 9.2 kΩ load. Takhedmit et al. [19] proposed a rectenna using a CP antenna for 2.45 GHz. 69% maximum efficiency and 1.1 V output voltage was measured for an optimized 2.5 kΩ load and 20 $\mu W/cm^2$ input power density.

In this work, initially a spurious free circular shaped antenna was used [20] for 2.45 GHz rectenna application. The antenna gain was found unsuitable for rectenna application. Therefore, it was loaded with an angle and polarization insensitive FSS. The FSS loaded antenna has high gain, which makes it suitable for rectenna applications. The antenna was connected with a 2.45 GHz matched rectifier to form

a rectenna circuit. An L-section matching network converts the complex rectifier impedance to 50 Ω antenna impedance.

2 2.45 Ghz Rectifier Design

SMS 7630-005LF Schottky diode has been used to design the rectifier circuit (Fig. 1(a)). 3 kΩ load is considered. Complex input impedance of the rectifier is plotted in Fig. 1(b) and is found to be Z_{in} = 26.95–j209.25 Ω at 2.45 GHz. Therefore, the rectifier is unmatched with typical 50 Ω antenna impedance. To achieve maximum efficiency, the rectifier has been impedance matched with the antenna using a L-section matching network. The matching network consists of a shunt inductor of 50.95 nH and a series inductor of 18.37 nH. After inserting the L-section matching network, Z_{in} becomes 52.06 + j2.45 Ω. To further improve the matching, a transmission line of width 4.61 mm and length 24 mm has been added between the L-section matching network and the source. This makes Z_{in} = 50.47 – j2.37 Ω. The 10 µF capacitor blocks the DC to reach source whereas 47µF capacitor bypasses the RF components to ground. The matched rectifier topology is shown in Fig. 1(c). Reflection and impedance data of the matched rectifier are plotted with frequency in Fig. 2. They reveal an acceptable matching at 2.45 GHz.

Efficiency (η) versus input power (P_{in}) plots of the matched rectifier at 2.45 GHz are shown in Fig. 3(a) for different load. It reveals that for 1, 2, 3 and 4 kΩ load maximum achieved efficiencies (η_{max}) are 67.2% for 10 dBm, 72.3% for 5.4 dBm, 73.03% for 3.05 dBm, and 72.5% for 1.4 dBm input power, respectively. Therefore, η_{max} remains almost constant with load variation. Efficiency and output voltage (V_{DC}) of the matched rectifier have been plotted with frequency in Fig. 3(b) for R_L = 3 kΩ and P_{in} = 3 dBm. It reveals maximum Efficiency of 73.03% at 2.45 GHz. Corresponding V_{DC} is 1.7 V.

The rectifier has been fabricated on a Rogers Duroid 5880 substrate of height 1.575 mm, tan(δ) = 0.0009, ε_r = 2.2, and copper thickness 0.035 mm, as depicted in Fig. 4(a). Figure 4(b) depicts details of fabricated rectifier circuit. The return loss measurement has carried out using a calibrated Keysight N5221A PNA. The measured frequency responses are shown in Fig. 5(a). The rectifier was measured to find the variation of V_{DC} and η with input power P_{in}. The 2.45 GHz frequency was generated using an Agilent E8257D signal generator and the load was set to 2.7 KΩ (nearest commercially available resistor of 3 kΩ). V_{DC} was measured using a volt meter. Efficiency was calculated for various P_{in} levels using Eq. (1) and η_{max} was found to be 53.03% at 3 dBm input power. Corresponding V_{DC} is 1.69 V. Measured V_{DC} and η plots are shown in Fig. 5(b). The difference between the simulated and measured efficiency is due to variations in diode parameters, parasitic effects of solder joints, and connecting wires that were not considered during simulation.

$$\eta = \frac{\mathrm{P_{dc}}}{\mathrm{P_{in}}} \times 100\backslash\% = \frac{\mathrm{V_{dc}^2}}{\mathrm{P_{in}R_L}} \times 100$$

1

3 Rectenna Design Using Circular Shaped Antenna

In order to develop the rectenna the spurious free 2.45 GHz antenna, reported in [20], is considered. The schematic diagram of the antenna is shown in Fig. 6. The rectangular ring slot on ground is used to suppress the spurious bands. The antenna is printed on a FR4 substrate of thickness 1.6 mm, area 30×35 mm^2, $\varepsilon_r = 4.4$, and $\tan(\delta) = 0.02$. The rectenna circuit is shown in Fig. 7. The rectenna has been measured to find output voltage (V_o) and efficiency variations with input/received powers in an anechoic chamber. Agilent E8257D signal generator was used as the 2.45 GHz signal source. The signal was amplified by a mini circuit ZX60-14012L RF amplifier (gain 11.9 dB) and fed to a horn antenna (gain 8 dBi at 2.45 GHz) using a cable (cable loss 3 dBm). The circular shaped antenna was used as the receiving element, which was kept at a far field distance (60 cm). Gain of the receiving antenna is 2.3 dBi at 2.45 GHz. Output voltages of the rectenna were measured by a volt meter across a 2.7 kΩ load for different transmitter powers (P_{in}) and measured data are plotted in Fig. 8(a). It reveals that V_o increases with P_{in} and the maximum output voltage of the rectifier is 190 mV for 10 dBm transmitter power. Efficiency of the rectenna have been plotted with incident/received power (P_r) in Fig. 8(b). It reveals that the rectenna has maximum efficiency of 1.24% for 1.1 mw incident/received power. Such low rectenna efficiency is not suitable for WPT applications.

4 Rectenna Design Using Fss Loaded Antenna

In this section, an attempt has been made to increase rectenna efficiency by loading it with a frequency selective surface (FSS). The concept is to design an FSS that is highly reflective at 2.45 GHz and place it at an optimized distance below the ground so that the backscattered field can be reflected by it and add with the broadside field at the same phase to increase the broadside gain. The increased gain will increase received RF voltage at the base of the antenna and hence efficiency of rectenna system.

A. Design of Frequency Selective Surface

The unit cell of the proposed FSS is shown in Fig. 9(a). Size of the unit cell is 12.9×12.9 mm^2 ($0.105\lambda_0 \times 0.105\lambda_0$, where λ_0 is free space wavelength at 2.45 GHz). Optimized dimensions of the unit cell are, d_1 = 10.2 mm, d_2 = 5.6 mm, and G = 0.65 mm. The FSS unit cell was simulated using CST Microwave studio (Version 14) with periodic boundary conditions (Fig. 9(b)) and incident EM wave from *z*-direction. For unit cell simulation the required boundaries are PEC on *yz*-planes and PMC on *xz*-plane. Wave ports are used on the plane of FSS (*xy*-plane). The final FSS structure is a 7×7 element periodic array of the unit cell and has dimensions 90×90 mm^2. 1.6 mm thick FR4 substrate with copper thickness 0.035 mm and $\varepsilon_r = 4.4$ is used to design the FSS. The FSS is four-fold symmetric and exhibits similar stop band response for TE and TM polarizations, as shown in Fig. 9(c). Transmission coefficient of the FSS has been simulated for TE and TM polarizations and are plotted in Fig. 10(a) and Fig. 10(b), respectively. They show angular insensitive performance of the FSS for both the polarizations. It is observed that both resonances are insensitive up to 70^0 incidence angle with a maximum frequency shift of 7.9 % only.

Equivalent circuit of the FSS is shown in Fig. 11(a). Values of the lumped elements can be found using [27] equations (2) and (3) and simulated $|S_{11}|$ response of the unit cell in Fig. 11(b). In the equivalent circuit, inductances represent metallic strips whereas the capacitances represent gap of the structure. Transmission line with characteristic impedance Z_0 represents the free space.

$$L = 2B_{3dB}|S_{11}(j\omega_0)|\eta_0/\omega_0^2 \quad (2)$$

$$C = 1/(2B_{3dB}|S_{11}(j\omega_0)|\eta_0) \quad (3)$$

where ω_0 is angular resonance frequency, B_{3dB} is the 3 dB bandwidth, $S_{11}(j\omega_0)$ is the value of S_{11} at ω_0, and η_0 is the free space impedance. The values of the lumped elements can be found as L_1 = 0.47651 nH, C_1 = 8.8559 pF, L_2 = 0.11989 nH, and C_2 = 2.2134 pF. The simulated $|S_{11}|$ responses of the unit cell and of its equivalent circuit are also plotted in Fig. 11(b) for comparison purpose.

B. FSS Loaded Circular Shaped Antenna

The FSS is placed below the antenna using four Bakelite rods, as shown in Fig. 12(a). Distance between the FSS and the antenna was determined using parametric analysis, shown in Fig. 12(b). It reveals that as H decreases from 35 mm to 20 mm, the antenna gain response improves till H = 25 mm and after that it deteriorates. Therefore, optimized distance 'H' is considered as 25 mm (or $0.204\lambda_0$). Radiation efficiencies of the antenna, with and without FSS loading, are plotted in Fig. 12(c) and is found to be 80.5% for unloaded antenna and 85% for loaded antenna. Comparison of the $|S_{11}|$ responses of the antenna with and without the FSS layer is shown in Fig. 13(a). It reveals that the loading of the FSS layer has minor effect on the $|S_{11}|$ response. The 10 dB RL bandwidth of the antenna covers 2.34–2.66 GHz. S-parameter and far field measurements of the antenna are done using a calibrated Keysight N5221A VNA. Comparison of the simulated and measured $|S_{11}|$ responses is provided in Fig. 13(a). They are in close agreement. The slight discrepancies at the higher frequencies are due to the parasitic effects of soldier joint of connector with antenna. Figure 13(a) reveals a 10 dB RL bandwidth of 2.20–2.51 GHz (around 6.58% on each side of the center frequency). Comparison of the gains of the antennas (with and without FSS layer) are provided in Fig. 13(b). It shows that within the 10 dB RL bandwidth, the gain of the FSS loaded antenna remains almost constant around 6 dBi with a maximum of 7.7 dBi at 2.45 GHz. It also reveals that the antenna gain is almost 3.34 times higher than that of antenna without FSS layer.

The normalized radiation patterns of the antenna, with and without FSS loading, on both the orthogonal planes at 2.45 GHz are provided in Fig. 14. Suppression of the back lobe is observed, as expected. Simulated half-power beamwidths at *xz* and *yz* planes are found to be 84^0 and 68^0, respectively. It also reveals that the cross-pol is more than 35 dB down than the co-pol at the broadside direction on both the orthogonal planes.

C. Development of the rectenna circuit

The fabricated rectenna is shown in Fig. 15. Efficiency of the fabricated rectenna can be calculated using the relation

$$\eta(\%) = \frac{V_{dc}^2}{R_L \times P_r} \times 100\%$$

4

where R_L is the load, P_r is the power received by the receiving antenna, and V_{dc} is the output DC voltage across load. The received power P_r can be calculated using the relation

$$P_r = \left(\frac{\lambda}{4\pi R}\right)^2 P_t G_t G_r$$

5

where P_t is the power at the input of the transmitting antenna, G_t is the transmitting antenna gain, G_r is the receiving antenna gain, λ is the free-space wavelength at 2.45 GHz, and R is the distance between the transmitting and receiving antenna.

The rectenna have been measured in an anechoic chamber to find the output voltage and efficiency variations with the transmitter (p_{in})/received (P_r) powers. Output voltages of the rectenna was measured by a volt meter across a load resistance 2.7 kΩ for different transmitter powers and measured data are plotted in Fig. 16(a). It reveals that output voltage of the rectenna increases with transmitter power till 7 dBm (output power of the signal generator) and after that it saturates. It further reveals that maximum output voltage of the rectenna is 1.52 V. The efficiencies of the rectenna have been calculated using Eqs. (4) and (5) and are plotted with received powers in Fig. 16(b). It reveals that the maximum efficiency of the rectenna is 66.13% for 1.1 mW received power (incident power at the antenna). This corresponds to a significant improvement in efficiency of the rectenna presented in section III, which has maximum efficiency of only 1.24 %.

Characteristics of the proposed rectifying antenna is compared with few other rectennas, available in literature, in Table I. It reveals that the proposed rectifying antenna has a high conversion efficiency at low input power than others.

Table I: Comparison of the input power and efficiency of the rectifier at frequency 2.45 GHz.

Ref. No	Rectifying element	Frequency (GHz)	Pin (dBm)	Efficiency (%)
[1]	HSMS 2862	0.9	7	60.0
[10]	HSMS 286C	2.45	-	51.5
[21]	HSMS 2820	2.4	10	56.7
[22]	HSMS 286C	2.29	10	< 50
[23]	MA4E1317	2.45	23	65
[24]	HSMS 2862	2.45	24	62
[25]	HSMS 2820	2.45	33	66
[26]	HSMS 2860	2.45	10	63
Proposed	SMS 7630	2.45	7	66.13

5 Conclusion

This paper presents the development of a 2.45 GHz rectenna for WPT application. Initially a matched rectifier was designed at 2.45 GHz using a L-section matching network. The output voltage of the rectifier at load was found to be 1.69 V. The maximum efficiency of the rectifier was measured to be 53.03% for an input power 3 dBm. Next, the rectifier was connected with a circular shaped antenna of gain 2.3 dBi to form the rectenna. The rectenna showed only 1.24% maximum efficiency. Since this efficiency is not acceptable for WPT application, next, an attempt was made to increase the rectenna efficiency by increasing the gain of the antenna. To accomplish this a 2.45 GHz reflector type FSS structure was developed and placed below the ground of the antenna at an optimized distance. The FSS reflected the backscattered wave which was then added with the radiated field in broadside direction in phase to result in gain enhancement. The FSS back antenna has 7.7 dBi gain and 85% radiation efficiency. The antenna was connected with the rectifier to form a new rectenna. The developed rectenna provided an output voltage of 1.52 V across the load resistor at 7 dBm input power (output power of the signal generator). The maximum achieved conversion efficiency was found to be 66.13%, which is much higher than the 1.24% maximum efficiency achieved earlier.

6 References

1. Ladan, S., Ghassemi, N., Ghiotto, A. and Wu, K. (2013). Highly efficient compact rectenna for wireless energy harvesting application. *IEEE microwave magazine*, 14(1), 117-122.
2. Han, Sang-Min, Ji-Yong Park, and Tatsuo Itoh. (2004). Active integrated antenna based rectenna using the circular sector antenna with harmonic rejection. *IEEE Antennas and Propag. Society Symposium,*

3. Ahn, Dal, J-S, Park, C-S. Kim, J. Kim, Y. Qian, and T. Itoh. (2001). A design of the lowpass filter using the novel microstrip defected ground structure. *IEEE Trans. Microw Theory Tech.*, 49(1), 86-93.
4. Radisic, Vesna, Y. Qian, R. Coccoioli, and T. Itoh. (1998). Novel 2-D photonic bandgap structure for microstrip lines. *IEEE Microw. And Guided Lett.,* 8(2), 69-71.
5. Liu, Z. Li, X. Sun, and J. Mao. (2005). Harmonic suppression with photonic bandgap and defected ground structure for a microstrip patch antenna," *IEEE Microw. Wireless Compon. Lett.*, 15(2), 55–56.
6. Hyungrak Kim, Kwang Sun Hwang, Kihun Chang and Young Joong Yoon. (2004). Novel slot antennas for harmonic suppression. *IEEE Microw. Wireless Compon. Lett.,* 14(6), 286-288.
7. Biswas, D. Guha and C. Kumar. (2013). Control of higher harmonics and their radiations in microstrip antennas using compact defected ground structures. *IEEE Trans. Antennas Propag.,* 61, 3349-3353.
8. Ma and G. A. E. Vandenbosch. (2014). Wideband Harmonic Rejection Filtenna for Wireless Power Transfer. *IEEE Trans. Antennas Propag.,* 62(1), 371-377.
9. Ramanujam, P., Venkatesan PG, R., Arumugam, C. and Ponnusamy, M. (2020). Design of a compact printed lowpass filtering antenna with wideband harmonic suppression for automotive communication. *Int J RF Microw Comput Aided Eng.* 30(12), e22452.
10. Huang, T. Yo, C. Lee and C. Luo. (2012). Design of Circular Polarization Antenna With Harmonic Suppression for Rectenna Application. *IEEE Antennas Wireless Propag. Lett.,* 11, 592-595.
11. A. Abbasi, and R. J. Langley.(2011). Multiband-integrated antenna/artificial magnetic conductor. *IET microwaves, antennas & propagation*, 5(6), 711-717.
12. Aboualalaa, A. B. Abdel-Rahman, A. Allam, H. Elsadek and R. K. Pokharel. (2017). Design of a Dual-Band Microstrip Antenna With Enhanced Gain for Energy Harvesting Applications. *IEEE Antennas Wireless Propag. Lett.,* 16, 1622-1626.
13. Shen, C. Chiu and R. D. Murch. (2017). A Dual-Port Triple-Band L-Probe Microstrip Patch Rectenna for Ambient RF Energy Harvesting. *IEEE Antennas Wireless Propag. Lett.,* 16, 3071-3074.
14. Nosrati, M., Dalili Oskouei, H. and Khalilpour, J. (2019). Parallel-series connected rectenna array using frequency selective surface (FSS) for power harvesting applications at 5.8 GHz. *Int J RF Microw Comput-Aid Eng.. 29*(9), 21819.
15. Brown. (1966). Experiments in the transportation of energy by microwave beam. *IRE International Convention Record*, New York, NY, USA, 8-17.
16. W. Yoo and K. Chang. (1991). 35 GHz integrated circuit rectifying antenna with 33% efficiency. *Electronics Lett.,* 27(23), 2117.
17. Ching-Hong K. Chin,Quan Xue, and Chi Hou Chan. (2005). Design of a 5.8-GHz Rectenna Incorporating a New Patch Antenna. *IEEE Antennas Wireless Propag. Lett.,* 4, 175-178.
18. Riviere, F. Alicalapa, A. Douyere, and J. D. Lan Sun Luk. (2010). A Compact Rectenna Deviceat Low Power Level. *Prog. Electromag. Res.,* 16: 137–146.

19. Takhedmit, L. Cirio, S. Bellal, D. Delcroix and O. Picon. (2012). Compact and efficient 2.45 GHz circularly polarised shorted ring-slot rectenna. *Electronics Lett.,* 48(5).
20. Pattapu, S. P. Biswal and S. Das. (2017). A 2.45 GHz DGS based harmonic rejection antenna for rectenna application. *USNC-URSI Radio Science Meeting*, San Diego, CA, 123-124.
21. Han, S.M., Park, J.Y. and Itoh, T. (2004). Active integrated antenna based rectenna using the circular sector antenna with harmonic rejection," *IEEE Antennas Propag. Society Symposium,* 4, 3533-3536.
22. Tawk, J. Costantine, F. Ayoub and C. G. Christodoulou. (2018). A communicating antenna array with a dual-Energy harvesting functionality. *IEEE Antennas Propag. Magazine,* 60, 132-144.
23. Ren, M. F. Farooqui and K. Chang. (2007). A Compact Dual-Frequency Rectifying Antenna With High-Orders Harmonic-Rejection. *IEEE Trans. Antennas Propag.,* 55(7): 2110-2113.
24. Heikkinen and M. Kivikoski. (2003). A novel dual-frequency circularly polarized rectenna," *IEEE Antennas Wireless Propag. Lett.,* 2, 330-333.
25. Hong, T. , Oh, K.M., Lee, H. W., Nam, H., Yun, T. S., Lee, D. S., Hwang, H. I. and Lee, J. C. (2010). Novel broadband rectenna using printed monopole antenna and harmonic-suppressed stub filter. *Microw. Opt. Technol. Lett.*, 52(5), 1194-1197.
26. Harouni, L. Cirio, L. Osman, A. Gharsallah and O. Picon. (2011). A Dual Circularly Polarized 2.45-GHz Rectenna for Wireless Power Transmission. *IEEE Antennas Wireless Propag. Lett.,* 10, 306-309.
27. V. M, Milka. M. P. and Dejan. V. T. (2017). Compact H-plane dual-band bandstop waveguide filter," *Journal of Computational Electronics,* 16, 939-951.

Figures

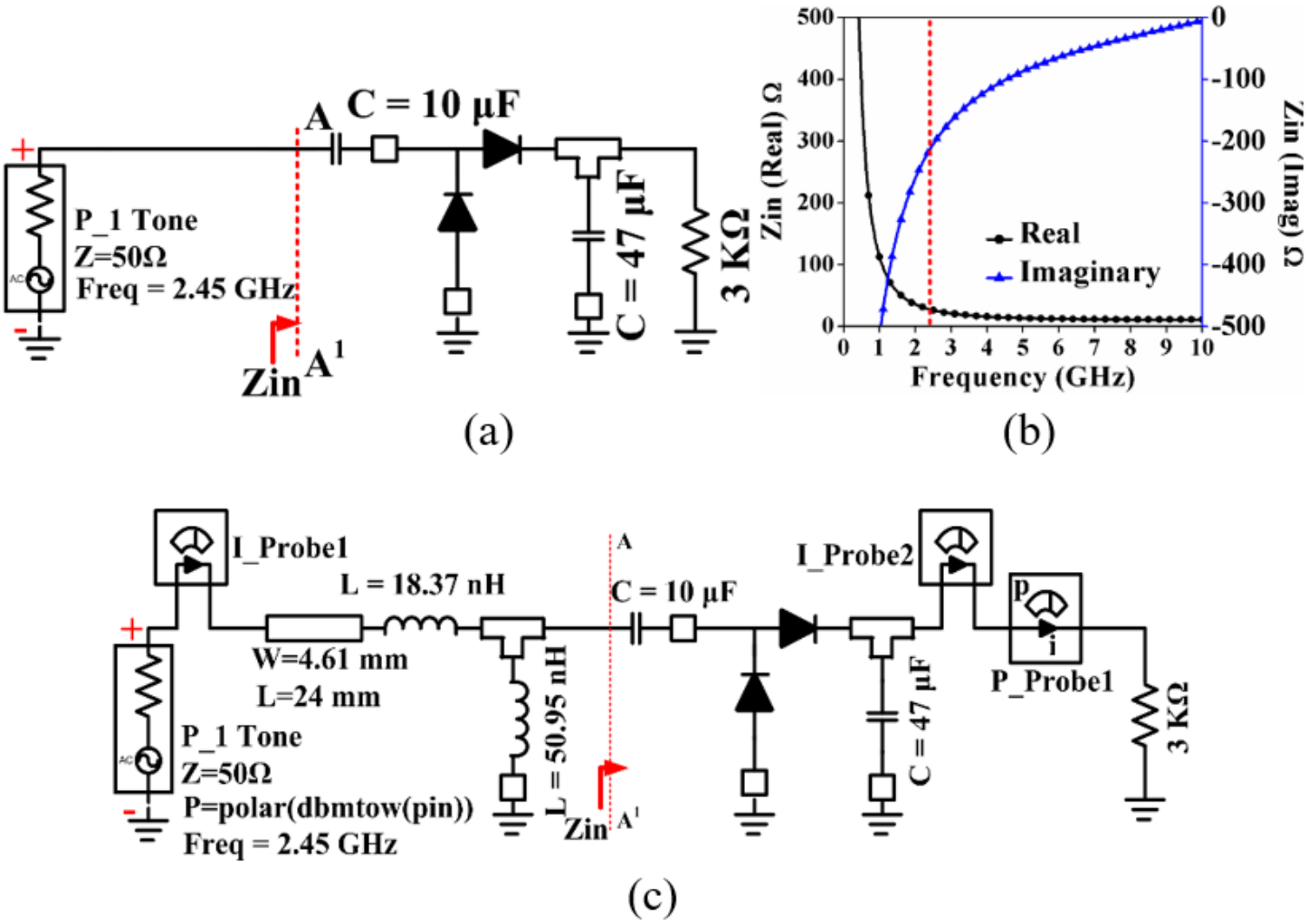

Figure 1

Typical rectifier circuit, (a). Unmatched rectifier, (b). Impedance of the rectifier, (c). A 2.45 GHz matched rectifier.

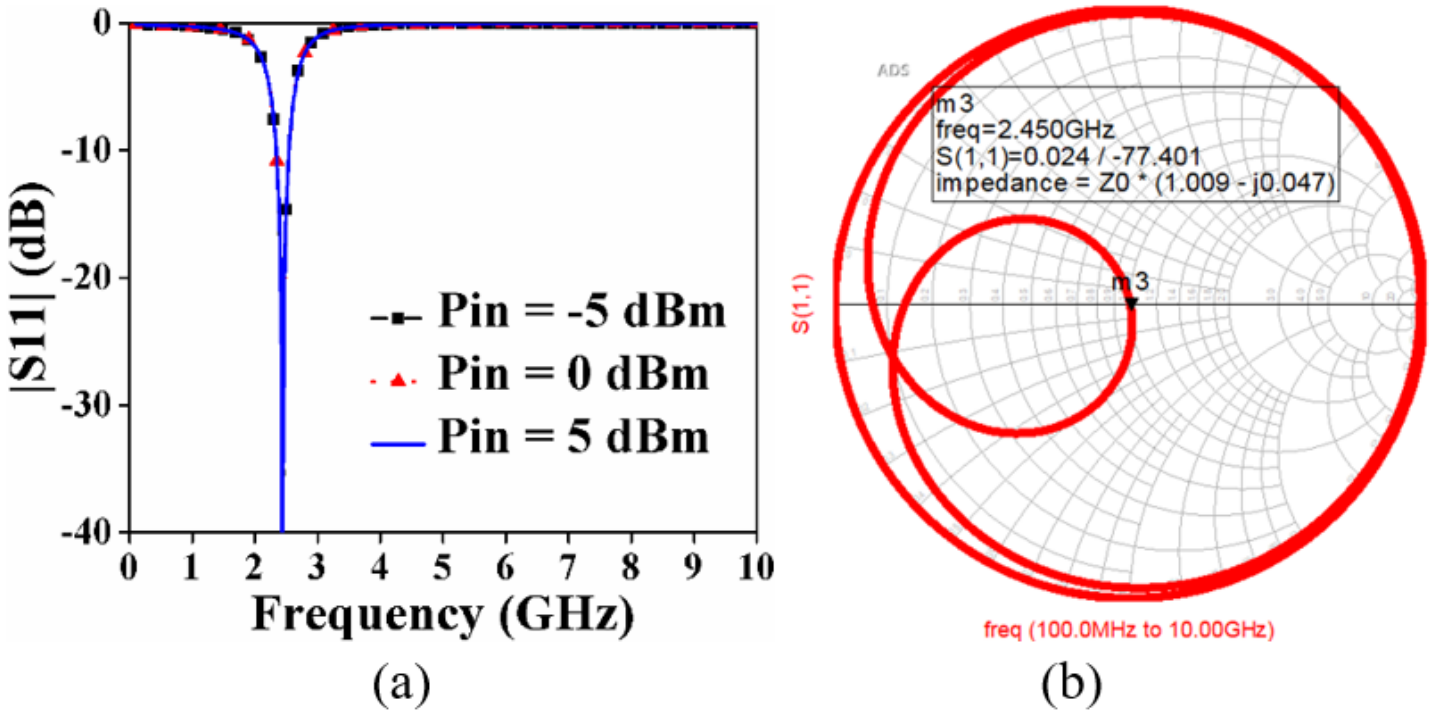

Figure 2

(a) Frequency response and (b) input impedance of matched rectifier

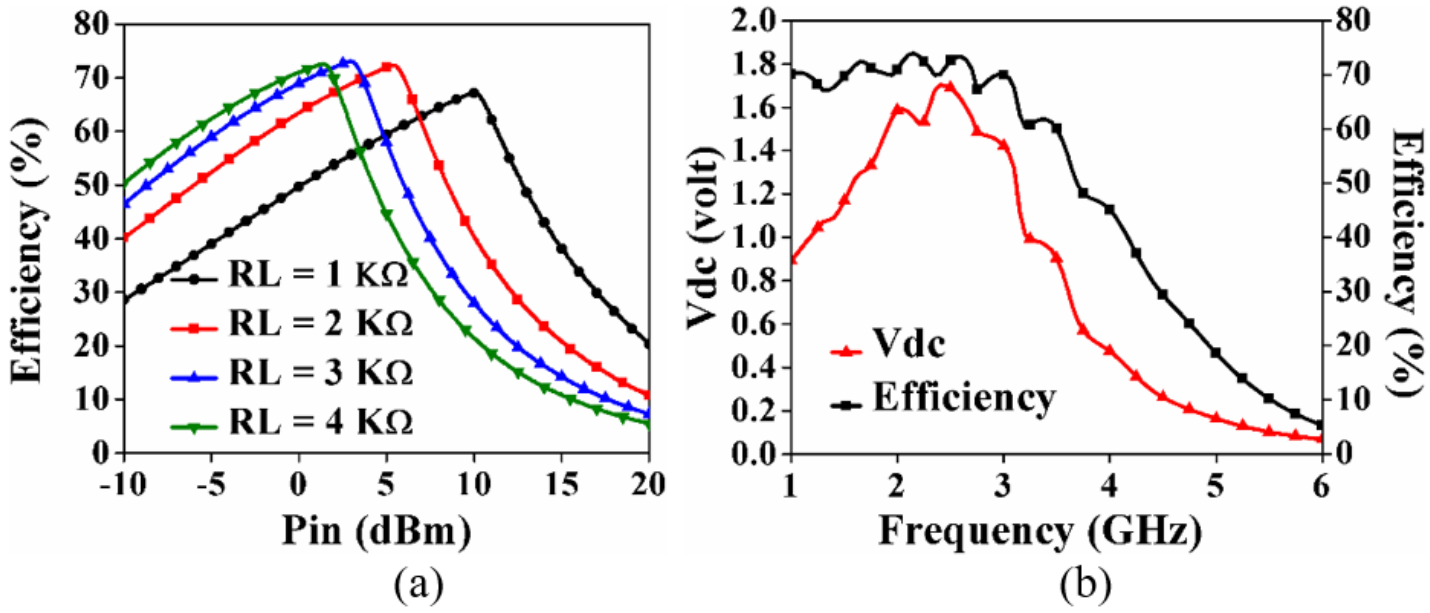

Figure 3

(a). Efficiency of the matched rectifier at 2.45 GHz for different load resistances, (b). Efficiency and output DC voltage of matched rectifier for RL = 3 kΩ and Pin = 3 dBm.

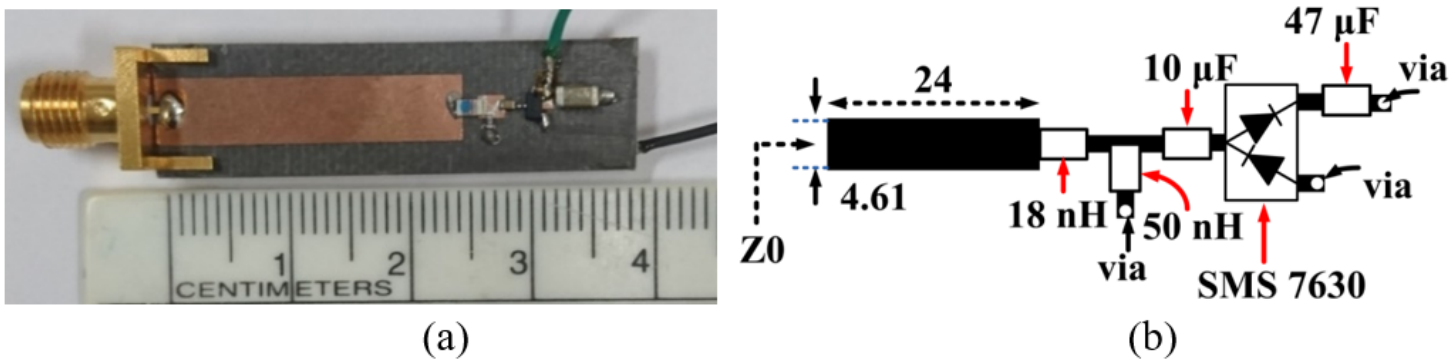

Figure 4

Fabricated matched rectifier. (a) Photograph, (b) circuit details.

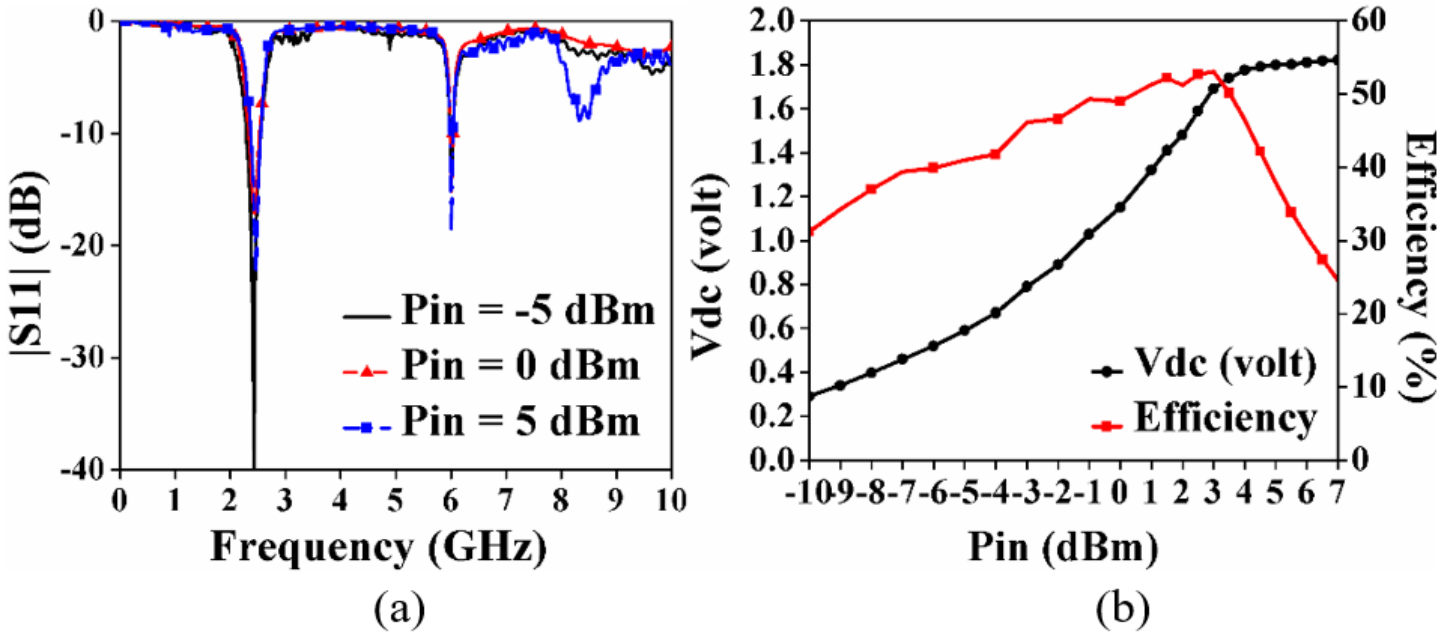

Figure 5

Measured rectifier results, (a). Frequency response of rectifier, (b). Output voltage and efficiency of matched rectifier.

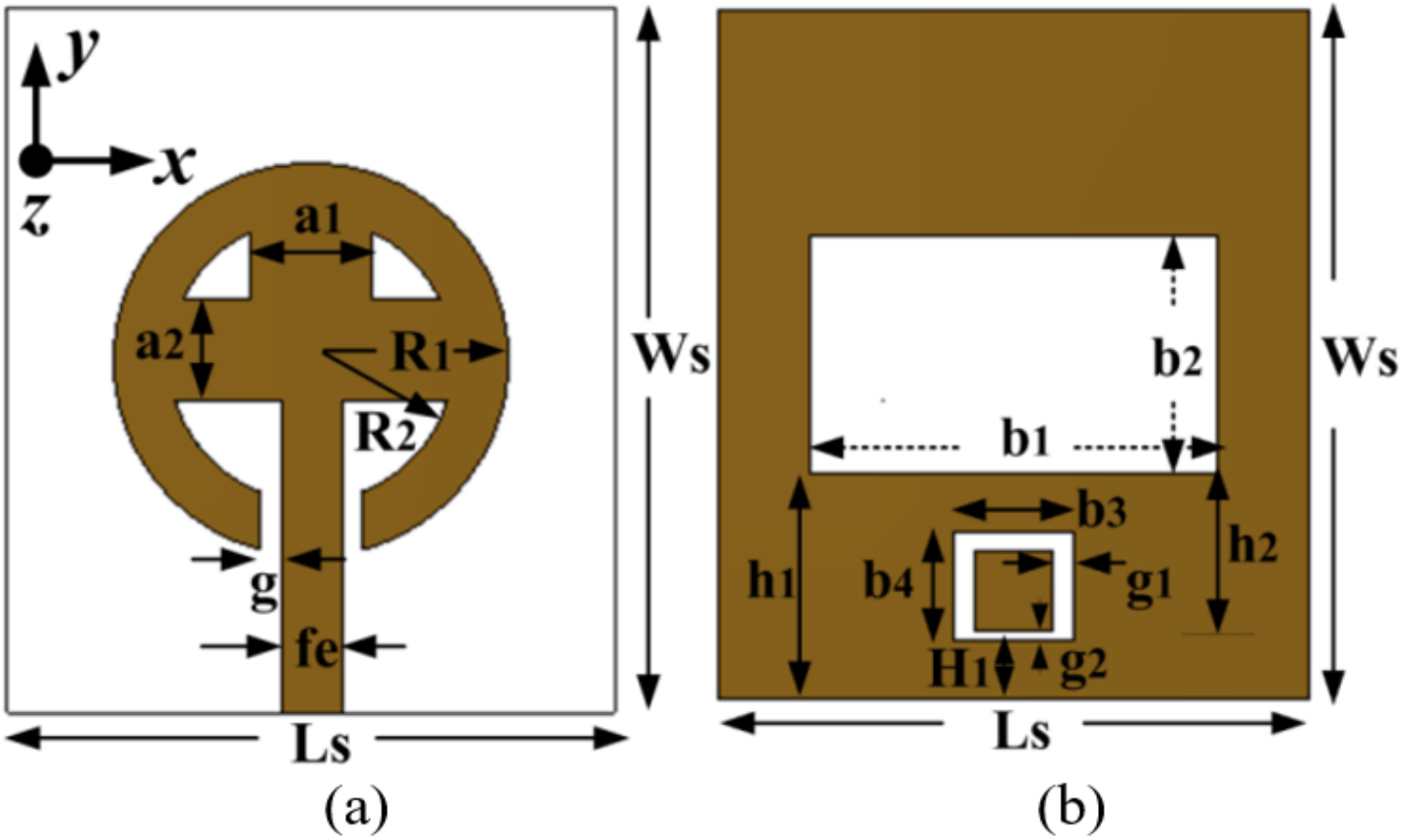

Figure 6

Schematic of spurious free circular-shaped antenna (a) radiator (b) ground. Ls = 30, Ws = 35, a1 = 6, a2 = 5, R1 = 9.75, R2 = 7, g = 1, fe = 3, b1 = 20.66, b2 = 12, b3 = 6, b4 = 5.5, h1 = 11.5, h2 = 8.5, g1=1, g2 = 0.5, H1 = 3 (all dimensions are in mm).

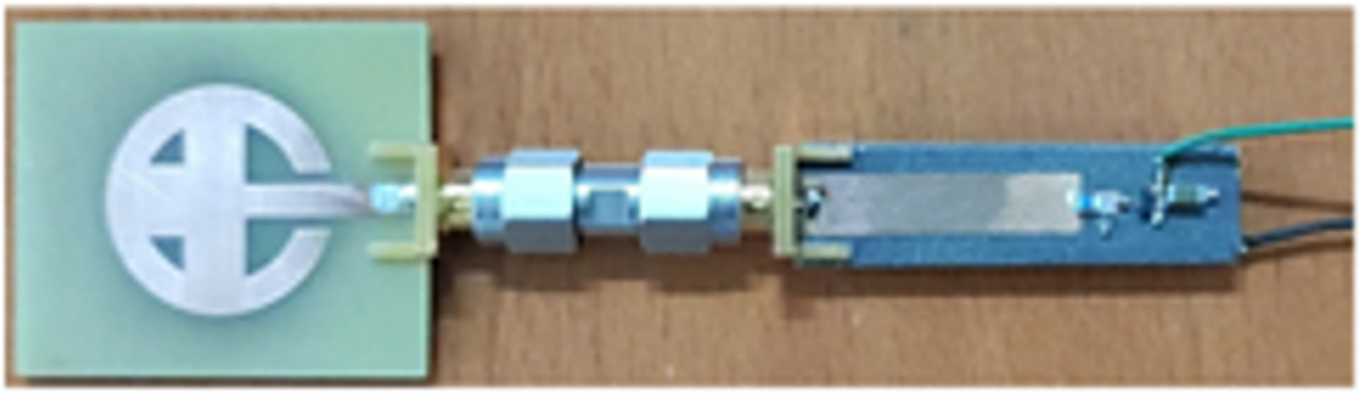

Figure 7

Circular shaped antenna based rectenna circuit.

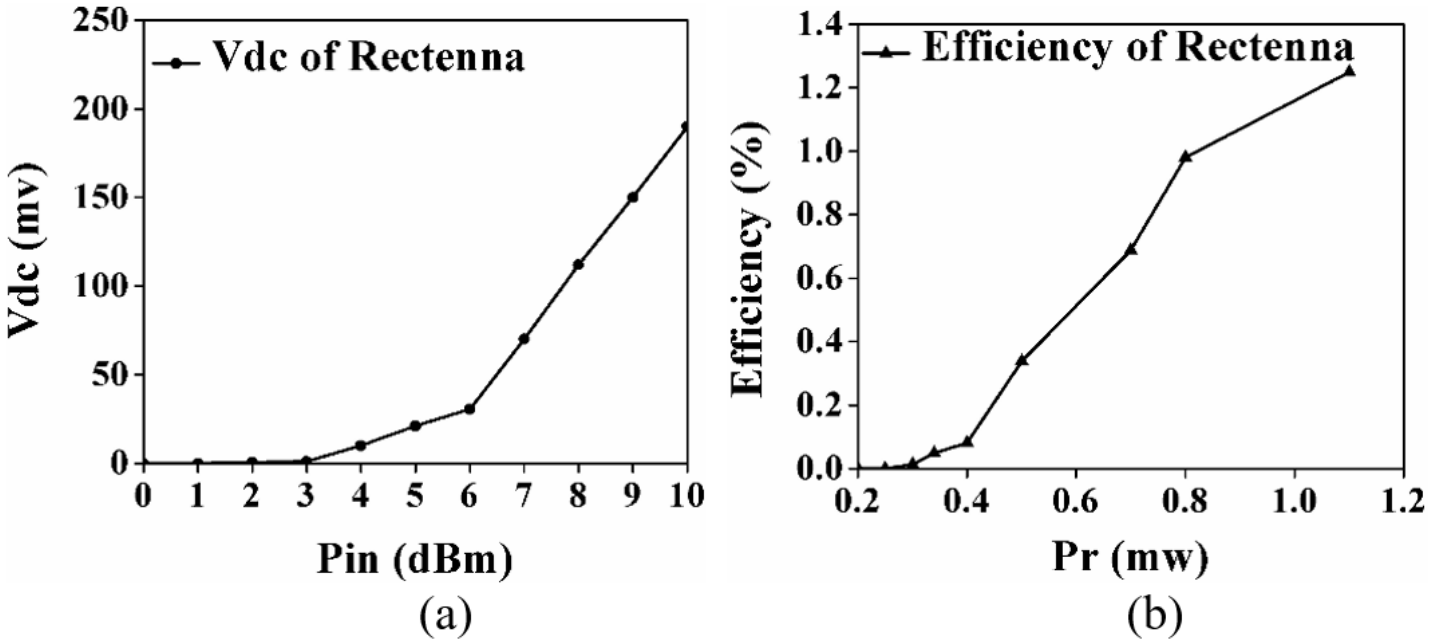

Figure 8

(a). Measured output voltage vs input power, (b). Calculated efficiency vs received power.

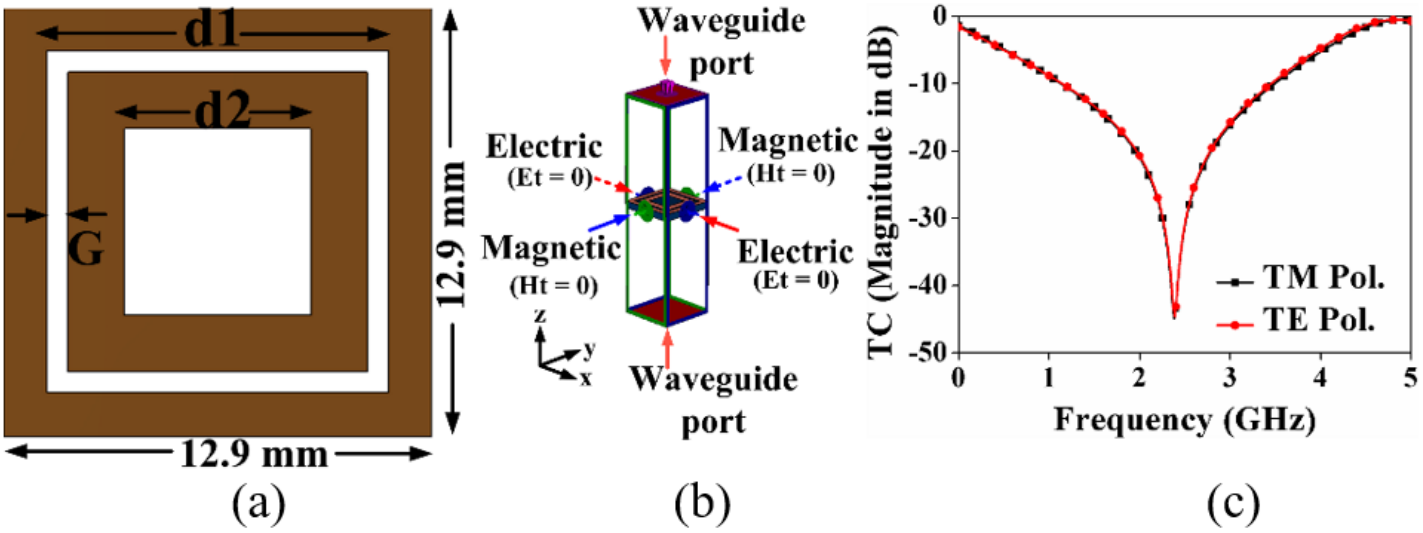

Figure 9

Proposed FSS (a) unit cell (d1 = 10.2 mm, d2 = 5.6 mm and G = 0.65 mm) (b) Unit cell boundaries, (c) TE and TM polarization of FSS.

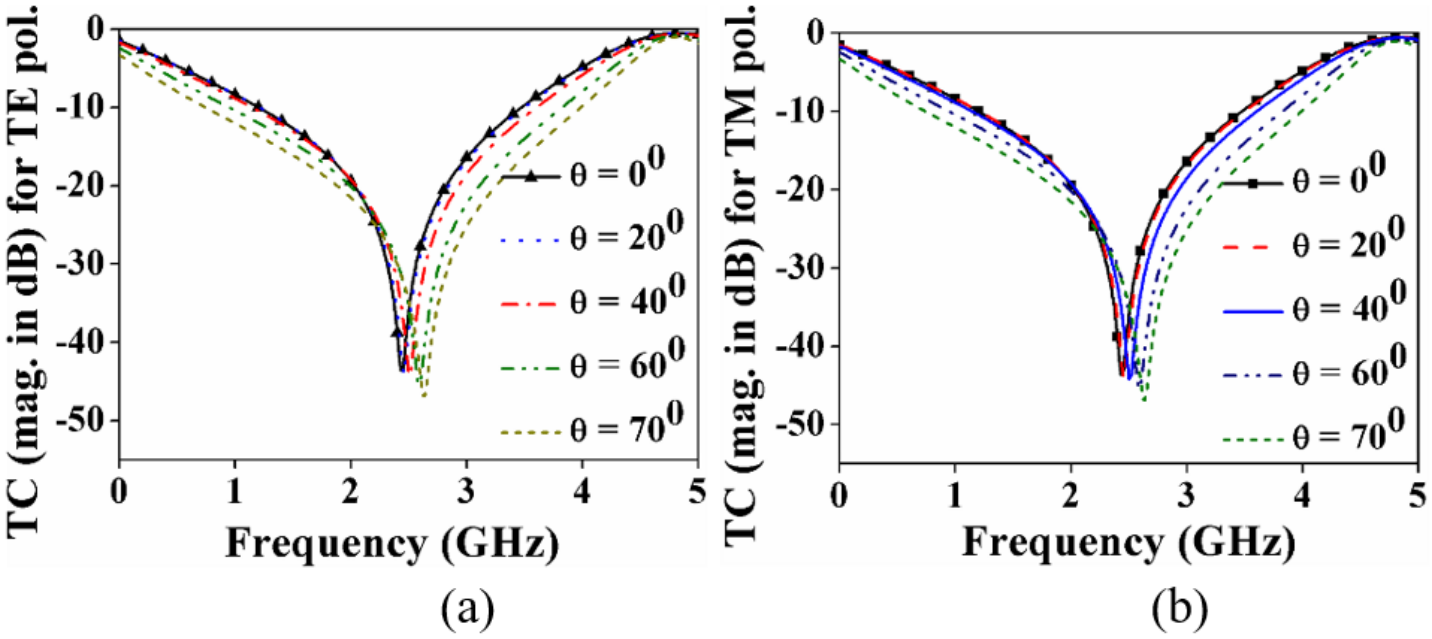

Figure 10

Transmission properties of FSS for different angle of incidence for (a). TE and TM polarization of FSS, (a). TE polarization, (b) TM polarization.

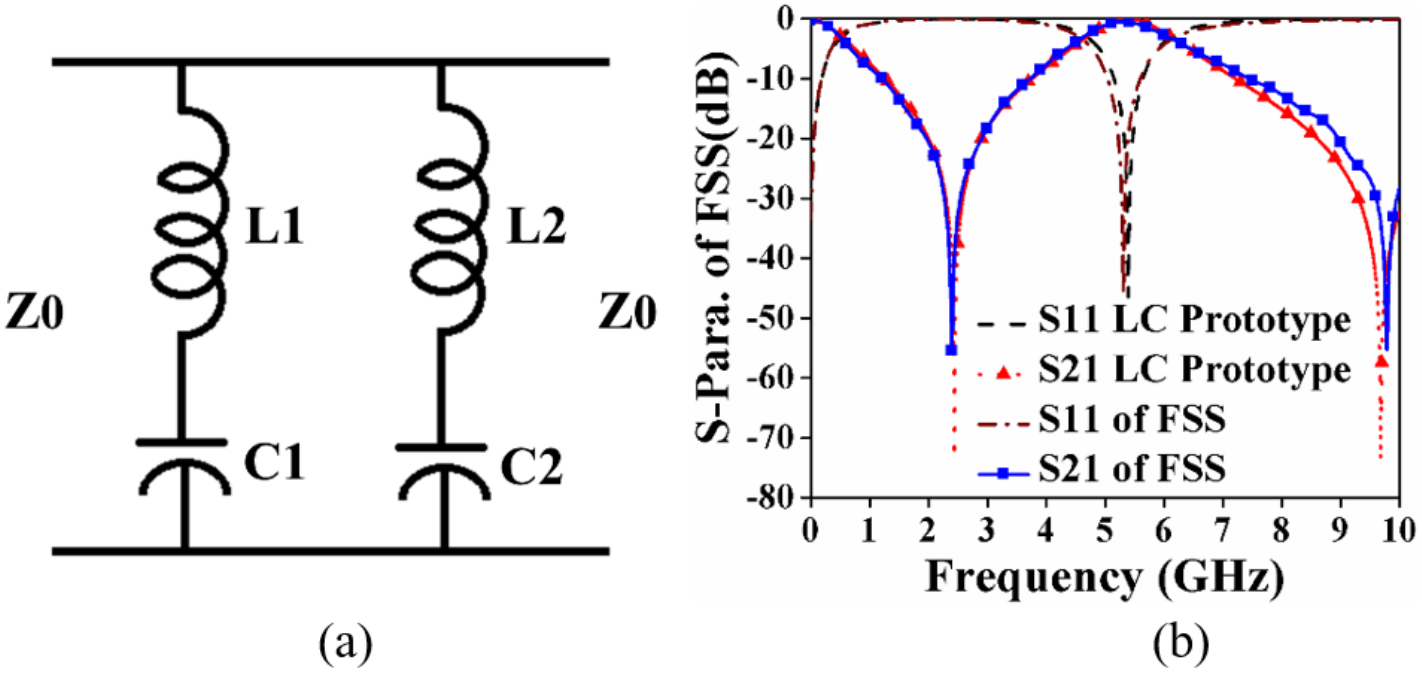

Figure 11

(a). Equivalent circuit model of the unit cell, (b). |S11| responses of the FSS unit cell and its equivalent circuit.

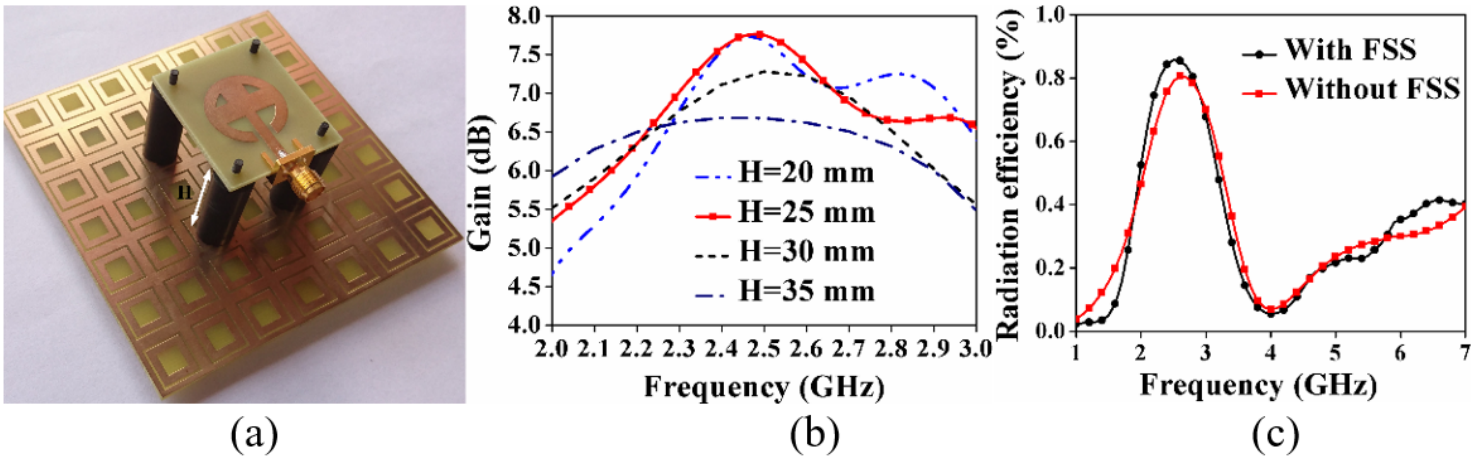

Figure 12

(a). Photograph of the FSS loaded antenna, (b). Gain responses for different H. (c). Radiation efficiency.

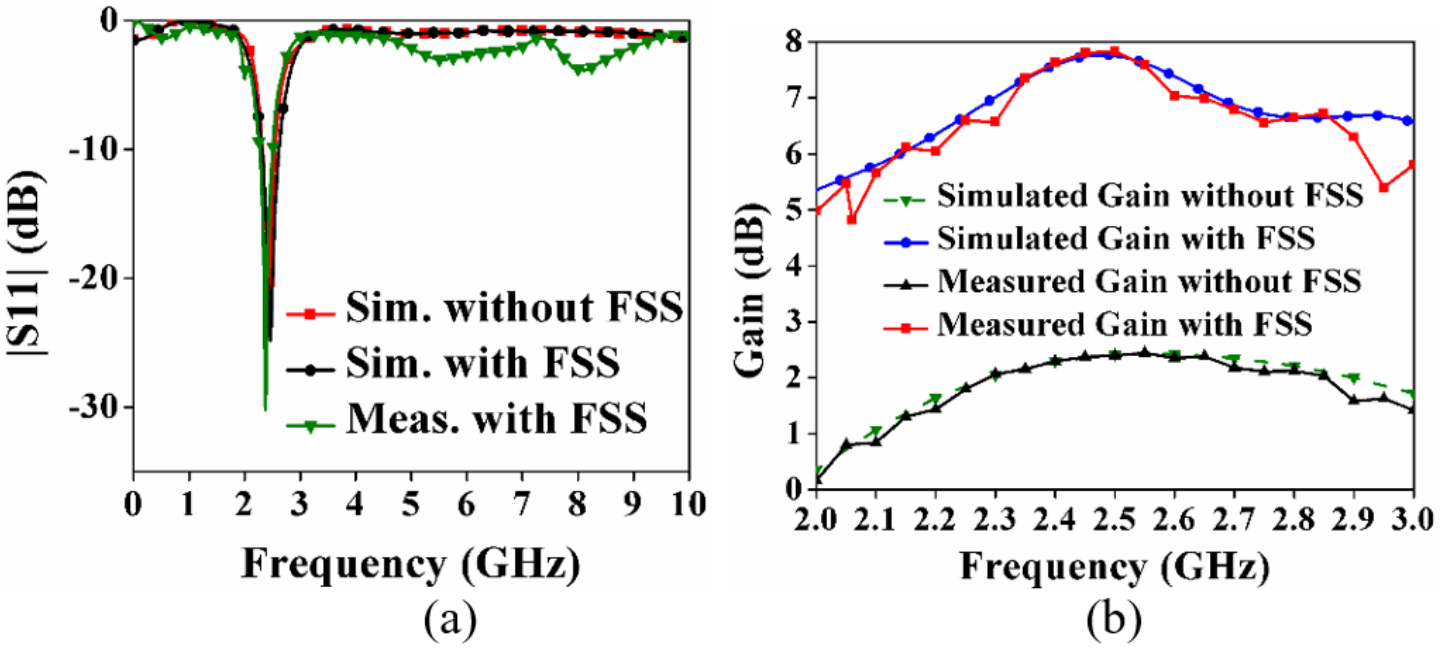

Figure 13

(a). |S11| response of the antenna, with (simulated and measured) and without FSS layer, (b). Gain response of the antenna with and without FSS.

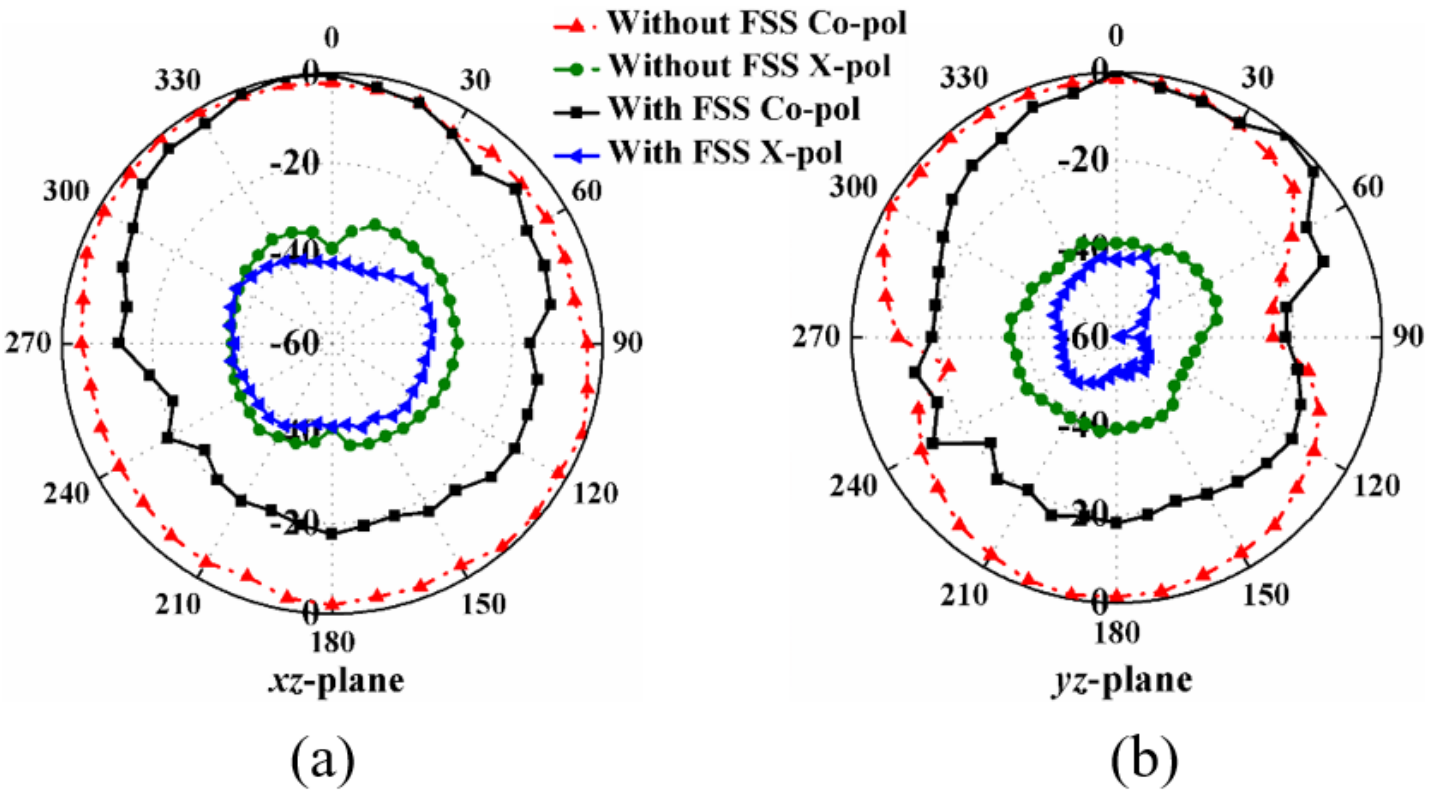

Figure 14

Measurement of normalized co- and cross-pol patterns of the with and with out FSS loaded circular-shaped patch antenna. (a). yz- and (b). xz-plane.

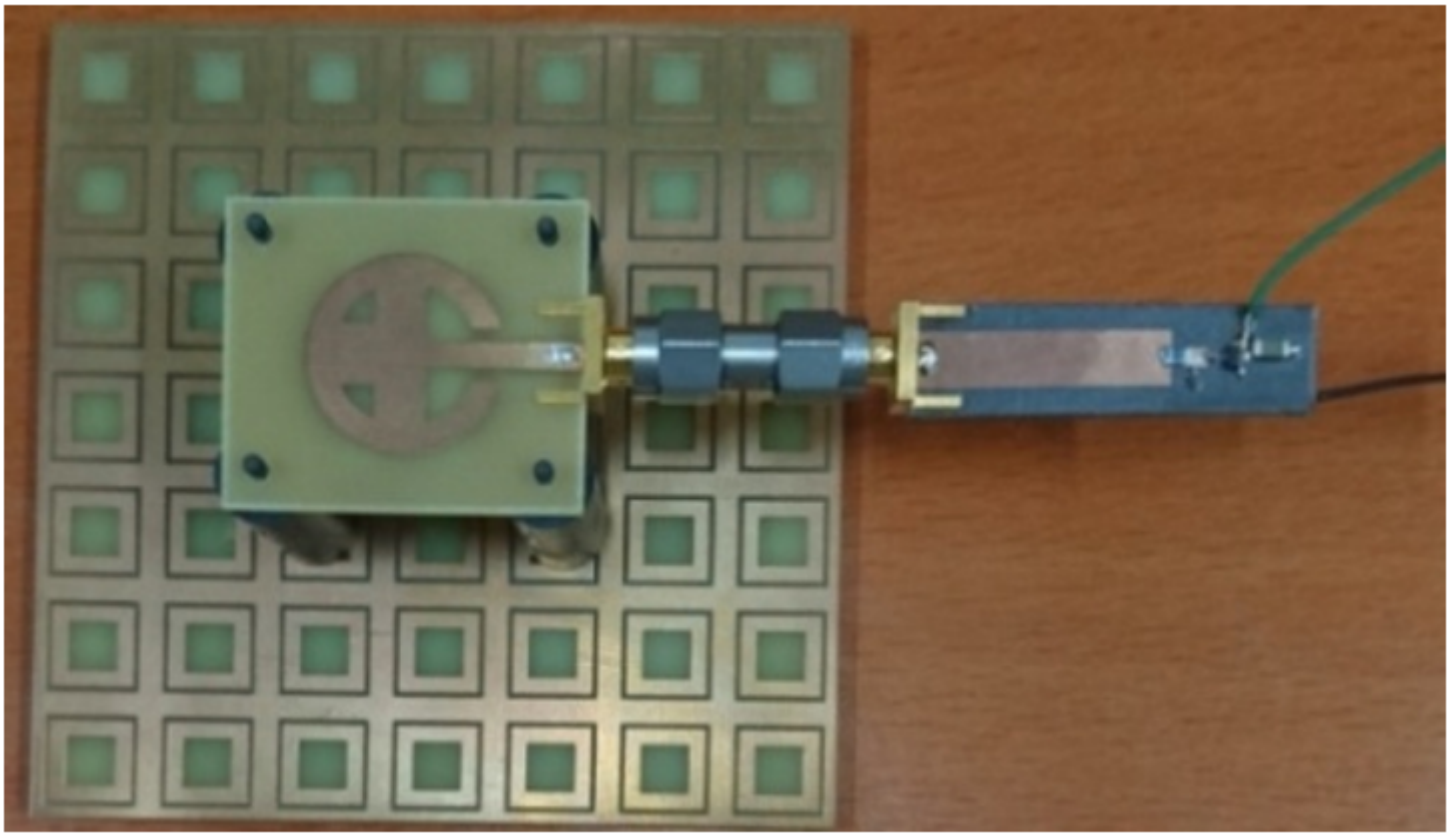

Figure 15

FSS backed circular shaped antenna based rectenna circuit.

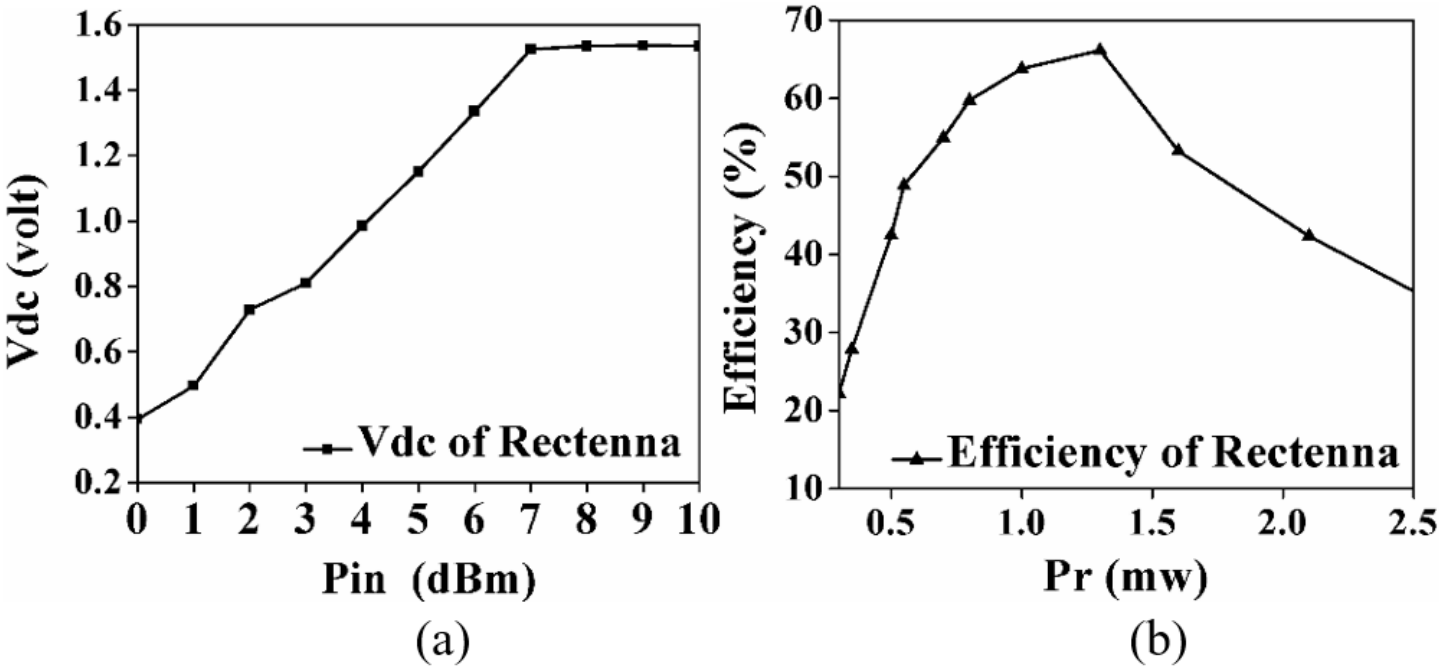

Figure 16

(a). Measured output voltage vs incident power for the rectenna. (b). Calculated efficiency vs received power for the rectenna.